Article published online: 2024-05-03

Review Article

Imaging of Benign Biliary Tract Disease

Samarjit Singh Ghuman[1] T.B.S. Buxi[1] Kinshuk Jain[2] Kishan S. Rawat[1] Anurag Yadav[1] Seema Sud[1]

[1] Department of CT and MRI, Sir Ganga Ram Hospital, Delhi, India
[2] Department of Radiodiagnosis, Sir Ganga Ram Hospital, Delhi, India

Indian J Radiol Imaging

Address for correspondence Kinshuk Jain, MBBS, DNB Trainee, Department of Radiodiagnosis, Sir Ganga Ram Hospital, Delhi, India (e-mail: kinshukjain12@gmail.com).

Abstract

This review article discusses the most common benign biliary disorders and the various radiological findings on multiple modalities. A broad spectrum of diseases including various congenital disorders, infective and parasitic etiologies, immunological pathologies such as primary sclerosing cholangitis, and immunoglobulin G4-related sclerosing cholangitis are discussed along with obstructive diseases and ischemic cholangitis. The article emphasized the imaging differential diagnosis of the above lesions as well as clinical correlates those that are most relevant to radiologists. The article briefly touched upon management and intervention where relevant.

Keywords

- cholangiopathy
- cholangitis
- IgG4-related sclerosing cholangitis
- PSC

Introduction

Bile is secreted by the hepatocytes into the biliary canaliculi which then coalesce to form subsegmental and segmental ducts and ultimately drain via the common bile duct into the duodenum.[1] Both benign and malignant lesions can involve the biliary tree. Patients almost always present with altered liver functions or jaundice and imaging usually reveals altered morphology of the biliary drainage system or the hepatic parenchyma.[2,3]

Development and Anatomy

The hepatic diverticulum arises from the ventral foregut during the fourth embryonic week. A thin double layer of cells is seen surrounding the portal vein during development of the liver, this is termed as the "ductal plate." Ductal plate malformations give rise to a variety of diseases including biliary atresia, Caroli disease, Meckel syndrome, and Alagille syndrome.[4,5]

The ducts of the right and left lobe usually follow a predictable pattern of union, although a number of variations have been described.[4,6] The normal common bile duct (CBD) measures 6 to 7 mm in patients aged 18 to 65 years.[7] Extrahepatic ductal diameter increases 1 mm per decade of life. Larger duct diameters are seen after cholecystectomy.[8]

Imaging Modalities

Ultrasonography (USG): Ultrasound is usually the first method for evaluation of suspected biliary disorders.[9] It is sensitive for biliary radical dilatation (85–95%)[10] and can usually depict the level of block and sometimes the cause of obstruction. It is, however, operator dependent and limited by body habitus.

Computed tomography (CT): Uses ionizing radiation and requires injection of intravenous contrast for optimal visualization of liver parenchyma and biliary tree. Exquisite for vascular anatomy and comparable to percutaneous transhepatic cholangiography (PTC) using minimum intensity projections (MinIPs) to visualize the biliary tree.[11] CT using biliary contrast agent (meglumine biotrexate) can be used to visualize the anatomy of the biliary tree.[11,12]

Magnetic resonance imaging (MRI) and magnetic resonance cholangiopancreatography (MRCP): MRI can easily visualize hepatic parenchymal changes and can evaluate the biliary anatomy. Hepatocyte-specific contrast agents are excreted into the biliary tree and can be used for evaluation of the

DOI https://doi.org/10.1055/s-0044-1786038.
ISSN 0971-3026.

Thieme Medical and Scientific Publishers Pvt. Ltd., A-12, 2nd Floor, Sector 2, Noida-201301 UP, India

biliary anatomy and variations. MRCP images can be acquired using either two-dimensional (2D) or three-dimensional (3D) heavily T2-weighted (T2W) images, which preferentially show fluid and suppresses the background. Most protocols use 2D and 3D MRCP, T2 and T2W fat sat, diffusion-weighted imaging (DWI), and pre- and postcontrast T1W images for comprehensive evaluation[2–4,13,14] (►**Fig. 1**).

Hepatobiliary scintigraphy is done using 99mTc hepatobiliary iminodiacetic acid (HIDA) which is cleared through the hepatobiliary system. It can be used for diagnosis of gallbladder (GB) disease, biliary atresia, demonstrating biliary leaks, and choledochal cysts (CDCs).[4,5]

Endoscopic retrograde cholangiopancreatography (ERCP) and PTC are rarely used as diagnostic tools in the present day. ERCP is usually combined with a therapeutic procedure such as stenting or with a brush biopsy. Diagnostic choledochoscopy can be done for strictures of the CBD and for targeting biopsy.[15] MRCP now has diagnostic accuracy comparable to ERCP[2] (►**Table 1**).

Table 1 Major causes of benign biliopathy

Congenital	Caroli disease, choledochal cysts, Alagille syndrome, cystic fibrosis
Obstructive	Choledocholithiasis with/without cholangitis, chronic pancreatitis, portal cavernoma cholangiopathy, primary sclerosing cholangitis
Immunologic	IgG4-related sclerosing cholangitis, eosinophilic cholangitis
Infective	Recurrent pyogenic cholangitis, AIDS cholangiopathy, parasitic cholangiopathy
Ischemic	Hepatic artery thrombosis, hematologic disorders, vasculitis, post therapy (TACE/TARE), secondary sclerosing cholangitis in critically ill patients, portal cavernoma cholangiopathy

Abbreviations: AIDS, acquired immunodeficiency syndrome; TACE, transarterial chemoembolization; TARE, transarterial radioembolization.

Congenital

Biliary Atresia

Biliary atresia is an inflammatory pediatric cholangiopathy causing fibrosis and obliteration of bile ducts, leading ultimately to biliary cirrhosis. It may be syndromic (associated with heterotaxy and polysplenia) or nonsyndromic. The primary differential diagnosis is neonatal hepatitis.

Ultrasound is the most common initial test and biliary dilatation is never seen. The "triangular cord sign" is

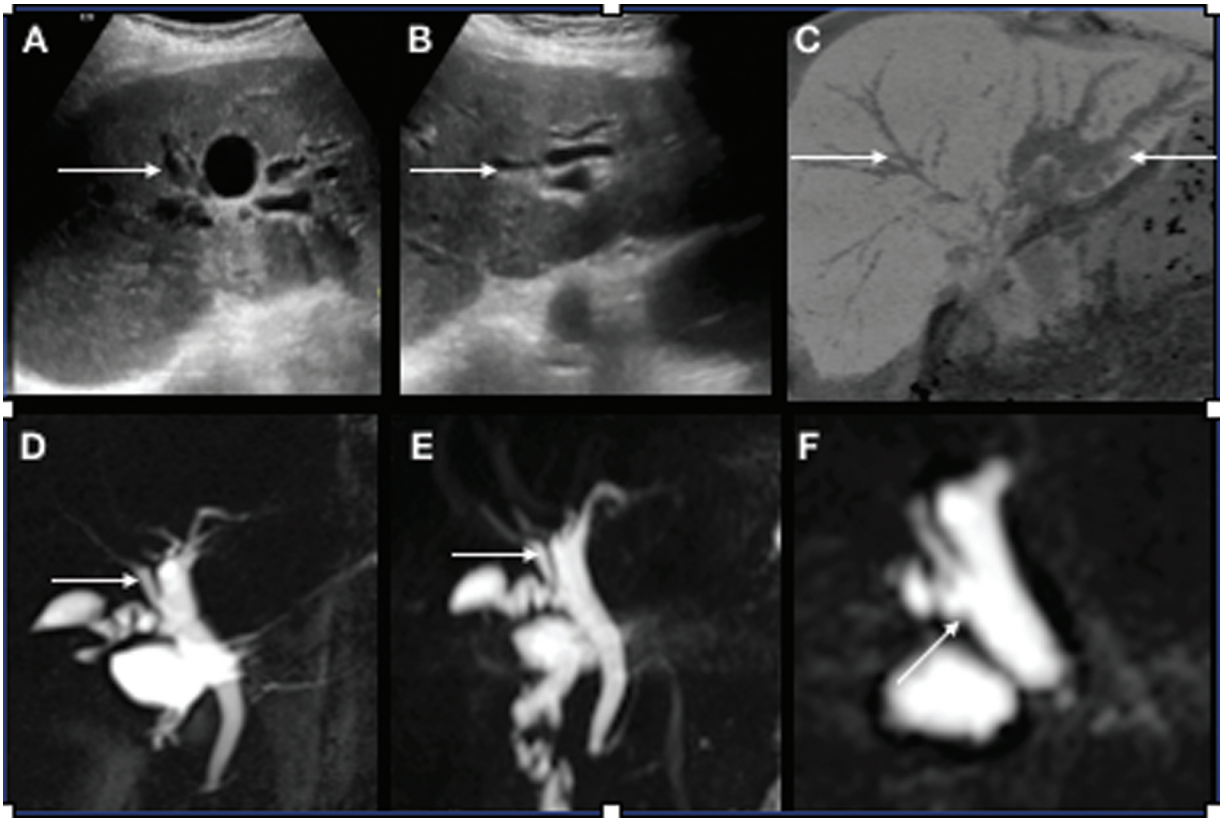

Fig. 1 A 49-year-old male with jaundice. Ultrasonography (USG) images showing linear hypoechoic tubular structures (arrows) converging toward the hilum in the right (**A**) and left (**B**) lobes—dilated intrahepatic biliary radicles (IHBRs). (**C**) Minimum intensity projection (MinIP) computed tomography (CT) images clearly showing asymmetrically dilated IHBR.(arrows). Thick (**D**) and thin (**E**, **F**) slab magnetic resonance cholangiopancreatography (MRCP) showing aberrant IHBR drainage (arrows). Right posterior duct is clearly seen to drain into the cystic duct insertion on the thin three-dimensional (3D) MRCP sequence. Ultrasound cases and figures : Courtesy of Dr. Deeksha Rastogi, Department of Ultrasound, Sir Ganga Ram Hospital, Delhi, India.

increased echogenic soft tissue measuring more than 4 mm anterior to the anterior wall of the right portal vein (80% sensitive, 98% specific). GB abnormalities include nonvisualization of the GB lumen, small GB (length < 15–19 mm), abnormal shape and wall of the GB, and no emptying of the GB after feeding. The "GB ghost triad" includes small GB, abnormal mucosal lining with indistinct wall, and knobby or irregular GB outline. Biliary atresia may be associated with macrocysts > 0.5 mm at the hepatic hilum or microcysts at the confluence, porta, or along the right portal vein. Increased hepatic subcapsular flow and hepatic artery diameter have been reported.

MRI has almost comparable sensitivity and specificity as ultrasound and findings include nonvisualized CBD, abnormal GB morphology, and increased periportal soft tissue > 5.1 mm. MRCP scan be useful to differentiate cysts associated with biliary atresia from CDCs.

Nuclear medicine using HIDA shows lack of excretion of the tracer into the bowel. In nondiagnostic cases PTC or biopsy may be used for confirmation[5,16,17] (►**Fig. 2**).

Choledochal Cysts

CDCs are cystic dilatation of the intra- or extrahepatic bile ducts or a combination of both. They are classified using Todani classification[18] I through V with isolated dilatation of the cystic duct proposed by some authors as type VI CDC. Type I CDC make up the majority of CDC and are further divided into type IA - cystic, IB - segmental, and IC - diffuse fusiform dilatation of CBD.

Type II CDCs are rare and seen as a diverticulum from the extrahepatic ducts. Type III CDC is also known as choledochocele and represents dilatation of the intraduodenal part of CBD.

Type IV CDCs are the second most common type of CDC making up 30 to 40% of CDC. Type IVA cysts have intra- and extrahepatic biliary dilatation and can be further classified into cystic-cystic, cystic-fusiform, and fusiform-fusiform types. Type IVB CDCs are rare and appear as multiple extrahepatic cysts[19] (►**Fig. 3**).

Pancreaticobiliary Maljunction

Though absolute values of 15 mm have been given for the length of the common channel, it was defined by the Japanese Biliary Association[20] as a congenital anomaly in which the pancreatic duct and bile duct join anatomically outside the duodenal wall leading to reflux and mixing of pancreatic and biliary juices. Patients with CDC type I (except IB) and type IVA almost always are accompanied by pancreaticobiliary maljunction (PBM). These patients have increased incidence of pancreatitis, biliary neoplasia, and CBD and GB stones. Morphologically, three types of PBM are recognized—PBM with right-angled junction, PBM with acute-angled junction, and complex PBM.

Caroli Disease

Congenital disorder characterized by irregular saccular or fusiform dilatation of the intrahepatic bile ducts. It may be diffuse, lobar, or segmental in distribution. It is a ductal plate

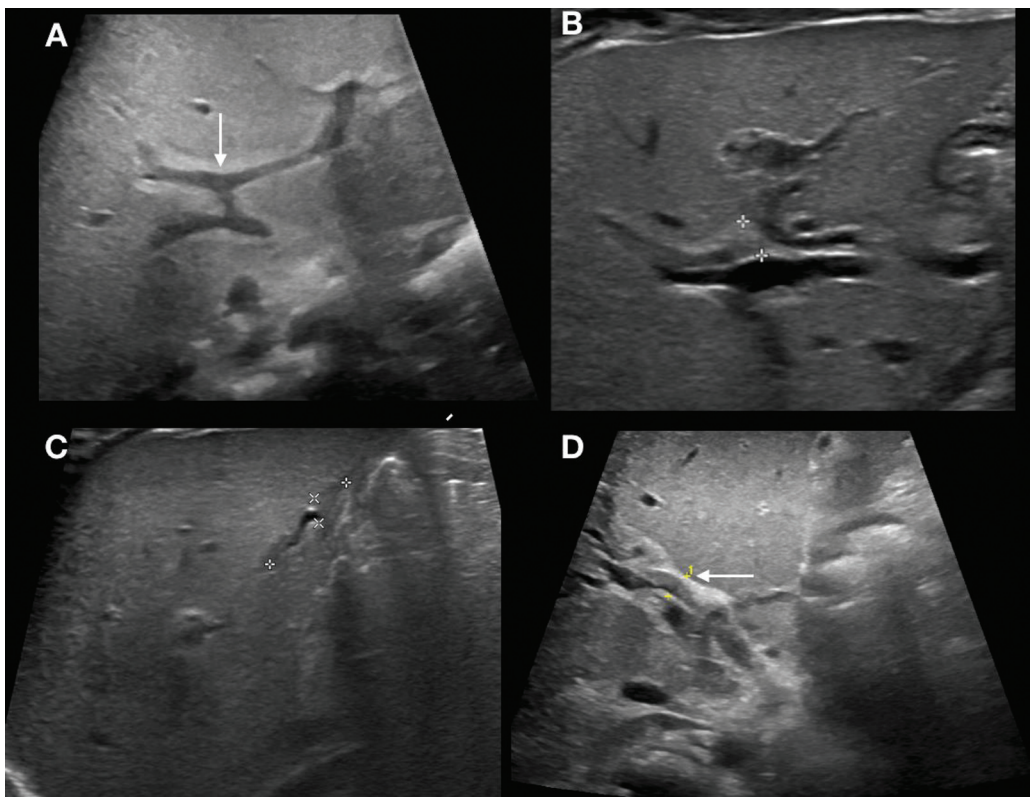

Fig. 2 Infant presented with clay colored stools and jaundice. Ultrasonography (USG) showing increased echogenicity anterior to portal vein division (arrow in **A** and calipers in **B**). Abnormal gallbladder shape calipers in (**C**) and increased diameter of hepatic artery 2.2 mm (calipers) in (**D**). Findings suggestive of biliary atresia.

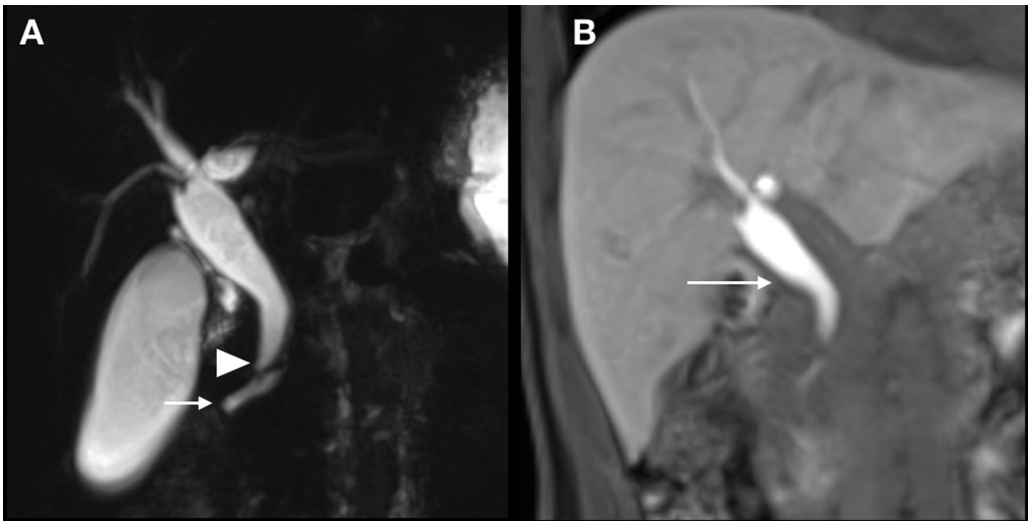

Fig. 3 Young child presented with abdominal pain. Ultrasonography (USG) showed dilatation of common bile duct (CBD). Magnetic resonance cholangiopancreatography (MRCP) was performed for further evaluation. Coronal MRCP images (**A**) showing fusiform dilatation of the CBD suggestive of choledochal cyst with narrowing at lower end (arrowhead) and pancreaticobiliary maljunction with long common channel (arrow). (**B**) Excretion of hepatobiliary contrast into the choledochal cyst (arrow).

malformation with autosomal recessive inheritance and more common in females, and when associated with hepatic fibrosis is known as Caroli syndrome. USG shows anechoic cystic lesions within the liver and associated calculi or sludge may be present. CT and MRI show multiple cysts with presence of the "central dot sign" which represents enhancing vascular radicles surrounded by dilated cystic biliary radicles. The differential diagnosis is polycystic liver disease. MR with hepatobiliary contrast agent will demonstrate excretion into the cysts in case of Caroli disease. Complications include cholangitis, abscesses, stones, malignancy, and secondary biliary cirrhosis[19] (►**Fig. 4**).

Obstructive

Choledocholithiasis

Choledocholithiasis is presence of stone in the CBD. Stones may cause biliary obstruction, cholangitis, and pancreatitis.

Abdominal ultrasound is usually the first modality used and has a reported sensitivity of approximately 73% and specificity of approximately 91%. Obesity, distal location of calculus stone, and lack of accompanying CBD dilatation can all reduce sensitivity of USG for calculus detection.[8]

Cholesterol calculi may not be seen on CT; however, calcified calculi and those with a nidus of gas within can be seen. CT can be used with biliary contrast agent.[12] The sensitivity of CT in detecting choledocholithiasis is 80%, ranging between 20 and 90% and use of MinIP may increase detection of calculi.[21]

MRCP is now the noninvasive diagnostic modality of choice for diagnosis of choledocholithiasis. Calculi appear as filling defects on a background of bright fluid. Both 2D and 3D MRCP sequences can be used, with 3D images being somewhat more sensitive for detection of stones. Calculi less than 5 mm in size or not surrounded by bile may be missed on MRCP.[21,22]

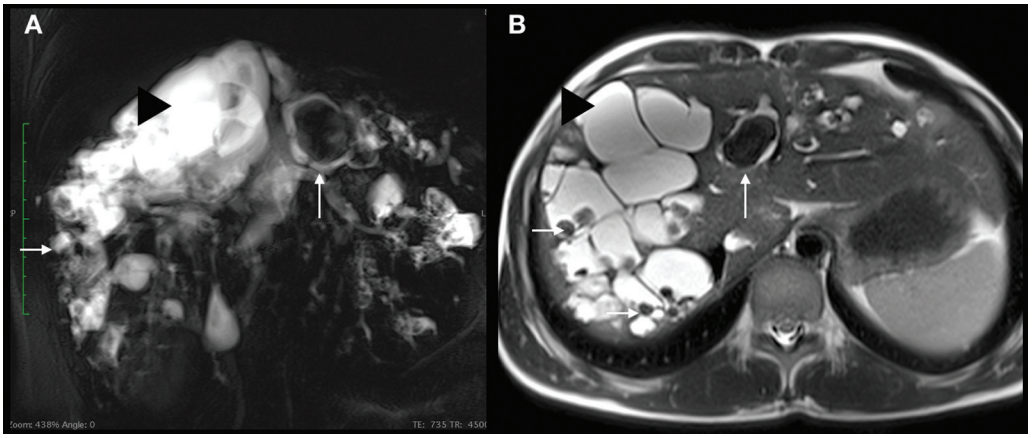

Fig. 4 A 16-year-old female with recurrent pain abdomen. Coronal thick slab magnetic resonance cholangiopancreatography (MRCP) (**A**) and axial T2-weighted (T2W) (**B**) images showing communicating dilated cysts (black arrowheads) consistent with findings of Caroli disease with multiple hypointense filling defects suggestive of calculi within (white arrows).

Pneumobilia may be confused with calculi. Air bubbles are generally ante-dependent and may show an air/fluid level, and "bloom" on the in-phase images. Hemobilia may appear dark on T2W images; however, will be hyperintense on T1W sequences. Vascular impressions may be misinterpreted as Hilar strictures; however, there will be lack of proximal dilatation.[22,23]

Endoscopic ultrasound (EUS) may provide higher diagnostic accuracy than MRI, with somewhat better sensitivity,[24] however, it is invasive.

Acute Cholangitis

Acute cholangitis (AC) occurs when biliary stenosis elevates pressure within the biliary system and causes spillover of bile and infection into the systemic circulation.[25,26] The Tokyo guidelines are useful for diagnosis (including imaging) and management of AC.[27]

Ultrasound may show dilated biliary radicles and CBD and may also show the cause of obstruction. Abscesses may be seen on USG.

CT and MRI demonstrate dilated ducts and are usually able to detect the cause of obstruction. Enhancement of the walls of the ducts may be seen, more commonly in the delayed images. Wedge-shaped, peripheral, or geographic areas of increased signal or enhancement may be seen. These findings have a high specificity in an appropriate clinical setting. Abscesses may be seen, which may appear clustered in a peribiliary location (cholangiolar abscesses). Portal vein thrombosis may occur in patients with cholangitis.[25,26] Treatment consists of removal of cause of obstruction and/or biliary drainage along with appropriate antibiotic therapy (►**Fig. 5**).

Portal Cavernoma Cholangiopathy

Portal cavernoma cholangiopathy (PCC) is defined as abnormalities in the extrahepatic biliary system including the cystic duct and GB with or without abnormalities in the 1st and 2nd generation biliary ducts in a patient with portal cavernoma. Presence of a cavernoma, typical cholangiographic findings, and absence of any other cause of cholangiopathy are required to arrive at this diagnosis. The mechanisms for findings of PCC include extrinsic compression of the bile ducts by the periportal vessels and biliary fibrosis secondary to ischemia related to thrombosis of tiny venules in the walls of the bile ducts.[28,29]

Fig. 5 A 55-year-old male with right hypochondrium pain and fever with chills. Coronal (**A**) and axial (**B**) computed tomography (CT) images showing dilated common bile duct (CBD) with tiny calculus at lower end (arrow in **A**) with asymmetrically dilated intrahepatic biliary radicle (IHBR) showing periductal hypodensity at places and ductal thickening (arrowhead in **B**). Axial CT images in arterial (**C**) phase showing dilated IHBR (arrowhead) with area of increased enhancement (arrow). Portal phase images show reduced attenuation around dilated IHBR in left lobe (arrowhead in **D**) consistent with findings of cholangitis.

Radiologic features of PCC include extrinsic indentation of the bile ducts, bile duct strictures, bile duct wall thickening, angulation and displacement of the extrahepatic bile duct, cholelithiasis, choledocholithiasis, and hepatolithiasis. In long-standing extrahepatic portal vein obstruction (EHPVO) peripheral atrophy of the liver may be seen due to reduced peripheral perfusion. Ultrasound with color Doppler can be used for evaluation of portal cavernoma formation, superior mesenteric and splenic veins, as well as evaluation of the intrahepatic ducts. CT also easily demonstrates EHPVO with associated findings and collaterals. Liver morphology alterations and transient hepatic attenuation differences may be seen after administration of intravenous contrast. Contrast-enhanced (CE) MRI with MRCP can easily demonstrate all the above findings as well, along with mural thickening of bile duct walls (►**Fig. 6**). Delayed duct wall enhancement may suggest fibrosis.

Classifications of PCC include morphological classification —classification by level of biliary obstruction and classification by severity of biliary abnormalities. Treatment includes biliary stenting, different forms of biliary drainage, and surgical shunts. PCC cholangiography may resemble a variety of entities including sclerosing cholangitis (SC) due to other causes and cholangiocarcinoma (CCA).[30]

Immunological

Sclerosing Cholangitis

SC are diseases which are associated with recurrent inflammation with progressive fibrosis and injury to the biliary system and imaging manifestations of bile duct stricturing. They may have a known cause (e.g., immunoglobulin G4 [IgG4] disease) or be idiopathic—primary SC (PSC).[2,31]

Primary Sclerosing Cholangitis

PSC is a disease of unknown etiology characterized by chronic progressive biliary inflammation and fibrosis leading to luminal narrowing and biliary strictures. It is associated with inflammatory bowel disease and is more common in males. The disease causes progressive hepatic fibrosis and cirrhosis and is associated with increased risk of malignancy including CCA, hepatocellular carcinoma, GB carcinoma, and colonic carcinoma. It has three subtypes—classic, (most common) small duct PSC, and PSC overlap with autoimmune hepatitis.[2,32–34] Diagnosis of PSC is made by typical cholangiographic findings and exclusion of secondary causes. The European Association for the Study of the Liver (EASL) guidelines recommend MRCP as the first option for imaging of suspected cases of PSC. Small duct PSC is diagnosed in patients with idiopathic cholestasis, normal imaging, and compatible histology. MRI is approximately 86% sensitive and 94% specific for diagnosis of PSC. The imaging hallmark of PSC is biliary strictures involving both intra- and extrahepatic ducts. The strictures are usually bilobar and multisegmental. Strictures are usually short, with variable upstream dilatation, which sometimes produce "beaded" appearance. Progressive fibrosis causes worsening of strictures with obliteration of peripheral ducts showing a "pruned tree" appearance. Diverticular outpouching of bile ducts is a characteristic finding that occurs in a minority of patients. Widening of the angles at the site of duct branching may be seen. Up to half the patients will show biliary mural

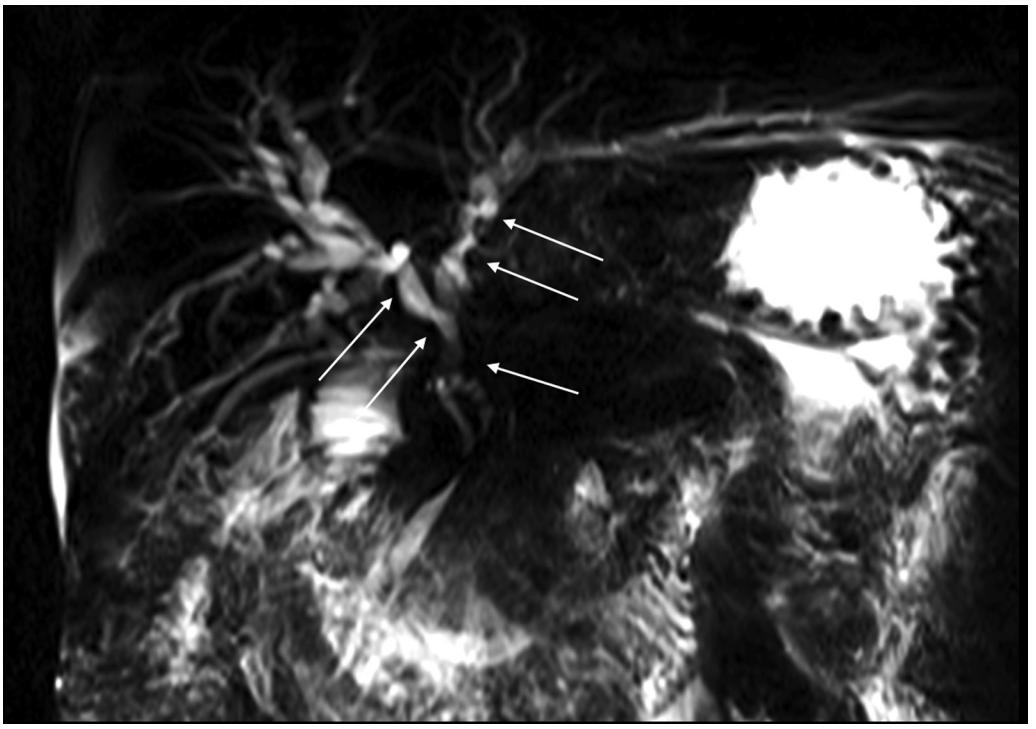

Fig. 6 Coronal magnetic resonance cholangiopancreatography (MRCP) images in a 45-year-old patient with extrahepatic portal vein obstruction (EHPVO) showing multiple extrinsic indentations on the right and left hepatic duct and the common bile duct (CBD), consistent with portal cavernoma cholangiopathy.

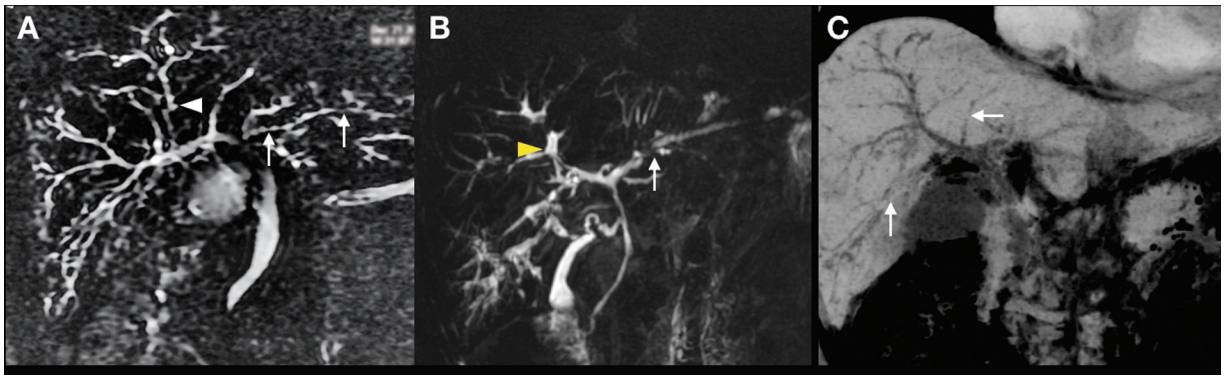

Fig. 7 A 45-year-old male, a known case of ulcerative colitis, presenting with fatigue and pruritus. Coronal magnetic resonance cholangiopancreatography (MRCP) images (**A**, **B**) showing cholangiographic findings of primary sclerosing cholangitis (PSC) with short segment strictures and irregularities shown by small white arrows. White arrowhead in (**A**) showing tiny diverticulae. Yellow arrowhead in (**B**) showing loss of acute angle at biliary branching. Note irregular outline of the biliary radicles and visualization of biliary radicles up to the periphery of liver. (**C**) Computed tomography (CT) with minimum intensity projection (MinIP) showing irregular dilatation of the bile ducts with small focal band-like strictures.

thickening ($>$ 2 mm) and enhancement. Isolated involvement of CBD is almost never seen. Intrahepatic stones may be seen. Strictures with more than 75% luminal narrowing are known as high-grade stricture. A dominant stricture is defined as a stricture with a luminal diameter of $<$ 1.5 mm in CHD or $<$ 1 mm in right or left duct, whereas a relevant stricture is any stricture associated with cholestasis or cholangitis.[35]

Signal intensity changes may be seen on T2W and DWI and these may or may not show associated enhancement. Morphological changes may be seen in the liver with segmental atrophy and caudate hypertrophy. Ultrasound may show dilated ducts; however, due to thickening, the duct may be obliterated and periductal fibrosis may prevent proximal ductal dilatation with normal appearing ultrasound. CT imaging may show irregular, discontinuous ductal dilatation, beading, irregularity, and thickening and enhancement around the ducts, as well as liver parenchymal changes (►**Figs. 7** and **8**).

Smaller duct involvement and calculi may be missed on CT.

Imaging is used to follow-up not only the primary disease in patients but also for development of malignancy. MRI-based risk scores[36] may predict risk of progression of patients. ERCP is used only as a problem-solving modality or for evaluation of suspicious strictures.

Approximately a third of patients with PSC who develop CCA will develop it within 1 year of diagnosis of PSC. The patients at risk for CCA are males with large duct disease and concomitant ulcerative colitis. Radiologically, most CCA develop from dominant strictures, and mass forming CCAs are less common in PSC. CE cross-sectional imaging should be performed when CCA is suspected followed by ERCP with sampling.[33] Presence of perihilar mass or periductal soft tissue that enhances maximally on delayed phase, with vascular encasement or hepatic invasion, with or without intraductal soft tissue is considered definitive for CCA in patients with PSC.[36] The definitive treatment for PSC is liver transplantation. The EASL reccomendation[32] for large duct PSC is to image yearly with USG and/or MRI for large duct PSC and image every 6 month for patients who have chronic liver

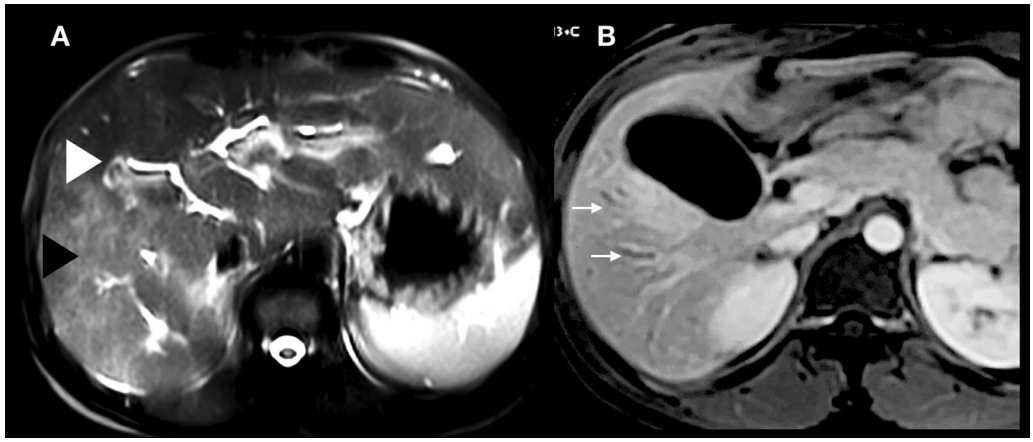

Fig. 8 A 55-year-old male with case of primary sclerosing cholangitis (PSC) on follow-up. Axial T2-weighted (T2W) images (**A**) showing increased signal (black arrowhead) in the hepatic parenchyma with a prominent caudate lobe. Note dilated biliary radicles (white arrowhead). Postcontrast images (**B**) in a different patient who presented with altered liver function tests (LFTs) reveal increased periductal enhancement (arrows) around the dilated biliary radicles.

Table 2 Findings of PSC

Demographics	Males > Females
Associated diseases	Inflammatory bowel disease
Cholangiographic abnormalities	Pruning, beading, skip dilatation, webs, diverticulae, calculi, strictures, lack of proximal dilatation
Signal and enhancement changes	Increased T2 and DWI signal, periductal enhancement, dysmorphia, cirrhosis
Complications	Cholangiocarcinoma

Abbreviations: DWI, diffusion-weighted imaging; PSC, primary sclerosing cholangitis.

disease. Liver elastography is suggested every 2 to 3 years (►**Table 2**).

IgG4-Related Sclerosing Cholangitis

IgG4-related sclerosing cholangitis (IgG4SC) is a disease of unknown etiology causing strictures in the biliary tree and is part of the spectrum of IgG4-related disease.[37] These patients have increased igG4 levels with dense infiltrates of IgG4 plasma cells and duct wall fibrosis.[38] Unfortunately, serum IgG4 levels may be raised in a number of pathologies including PSC and malignancy as well.

The HISORT criteria by Ghazale et al[39] and the Japanese Clinical Diagnostic Criteria 2012 and reviewed in 2020 are used for diagnosis of IgG4SC.[40,41]

Note that 87 to 92% of the cases of IgG4SC are related with autoimmune pancreatitis (AIP), in which the pancreas shows typical findings of type 1 AIP—fusiform "sausage" shape, peripancreatic halo, lack of main pancreatic duct (MPD) dilatation, reduced T1 signal, tapering of MPD, and usually diffusion restriction[42] (►**Fig. 9**).

Nakazawa et al[43] proposed a cholangiographic classification for IgG4SC based on the pattern of biliary involvement—type 1 - lower CBD stenosis, type 2a - intrahepatic stricture with dilation, 2b - intrahepatic stricture without dilatation, type 3 - Hilar and lower CBD stricture, and type 4 - Hilar stricture. Type 3 and 4 patterns of involvement may need additional investigations including ERCP for ruling out other pathology including CCA (►**Fig. 10**). Involvement of other organs including salivary glands, kidneys, and retroperitoneum may be seen. MR findings include thickening of the walls of the bile ducts with relatively preserved/visible lumen, long segment involvement, funnel-like narrowing, preferential involvement of lower end of CBD, and occasionally prestenotic dilatation. Bile duct thickening is relatively hypointense on T2 and diffusion restriction is usually seen. Homogenous enhancement of the thickened segments of bile ducts is seen (►**Fig. 11**). Associated GB wall thickening may be seen in 50% of patients.[2,31,41]

CECT may show similar findings as MR in the ductal system and may also show the findings of AIP, renal, and GB involvement. USG may pick up bile duct strictures and wall thickening, EUS and intraductal ultrasound show preserved mucosa with thickened walls showing vessels within.

In contradistinction to PSC, the disease responds well to steroid therapy. Response to steroid therapy is assessed by imaging and this should be done within 2 weeks of initiation of therapy[41] (►**Table 3**).

Eosinophilic Cholangitis

Eosinophilic cholangitis is a benign disease defined by eosinophilic infiltration in the walls of the bile ducts. It is associated with hypereosinophilic syndrome, allergic and parasitic conditions, and may be associated with eosinophilic gastroenteritis. Cholangiographic findings include segmental or diffuse thickening of the bile ducts with multifocal stricturing, which may be difficult to differentiate from PSC.[44] Involvement of the GB and cystic duct may be seen.[45] The disease responds well to steroid therapy.

Infective

Recurrent Pyogenic Cholangitis

Recurrent pyogenic cholangitis (RPC) is endemic in Southeast Asia including India. The proposed etiology for the disease is

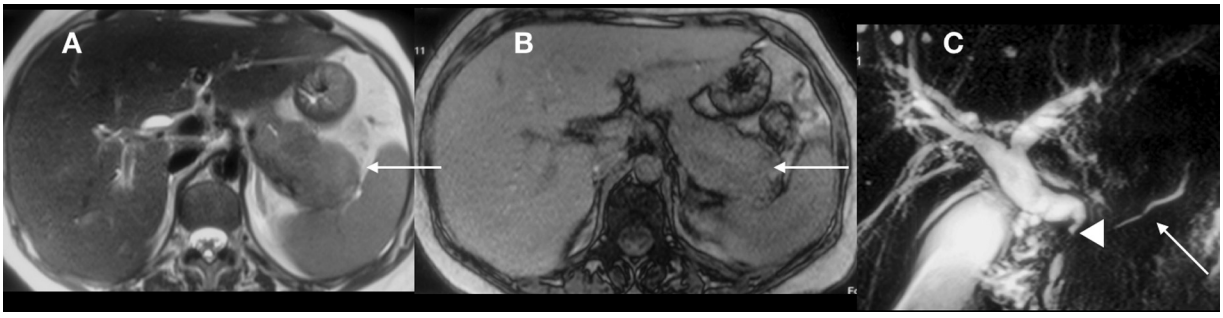

Fig. 9 A 45-year-old male with pain abdomen and altered liver function test (LFT). Axial T2-weighted (T2W) (**A**) and T1W (**B**) images show typical fusiform enlargement of the pancreas (arrows) which shows increased T2 and decreased T1 signal. Coronal magnetic resonance cholangiopancreatography (MRCP) (**C**) images show narrowing at lower end of common bile duct (CBD) (arrowhead), with mildly dilated irregular main pancreatic duct (MPD). Findings are suggestive of autoimmune pancreatitis, confirmed on biopsy.

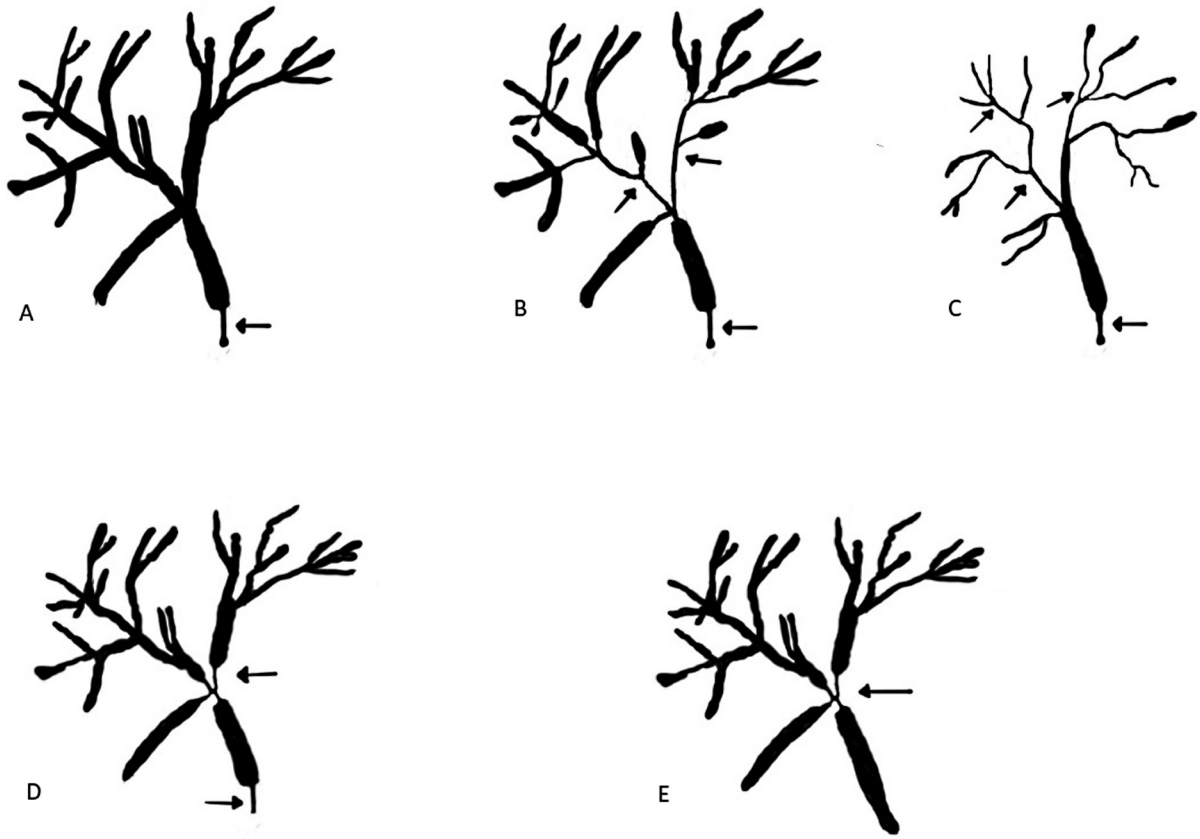

Fig. 10 Classification of immunoglobulin G4-related sclerosing cholangitis (IgG4SC) based on pattern of biliary tree involvement: (**A**) type 1 - lower common bile duct (CBD); (**B**) type 2A - intrahepatic with prestenotic dilatation; (**C**) type 2B - intrahepatic without prestenotic dilatation; (**D**) type 3 - Hilar and lower CBD involvement; (**E**) type 4 - Hilar involvement. Illustrations modified from Nakazawa et al. Digital Artwork by Dr. Varun Holla, Department of Radio Diagnosis, Sir Ganga Ram Hospital, Delhi, India.

Fig. 11 A 37-year-old female patient with immunoglobulin G4-related sclerosing cholangitis (IgG4SC). Axial (**A**) contrast-enhanced computed tomography (CECT) showing dilated intrahepatic biliary radicle (IHBR) (arrows) with thickened, enhancing walls. Coronal (**B**) CECT images showing thickened enhancing common bile duct (CBD) walls (arrows) with lumen seen despite the thickened walls.

infestation by parasites such as *Ascaris lumbricoides* and *Clonorchis sinensis*. Chronic inflammation results in fibrosis and infiltration of bile duct walls and portal tracts leading to biliary strictures. The hallmark is marked central and extrahepatic biliary dilatation with associated large pigment calculi in the intrahepatic and extrahepatic ducts. Impacted calculi in the ducts can lead to complete nonvisualization of the ducts —"the missing duct sign"[45] (►**Fig. 12**).

Decreased arborization and caliber of peripheral ducts are seen leading to arrowhead-shaped ducts. Segmental parenchymal atrophy, abscesses, bilomas, and portal vein thrombosis may be seen.[46] Ductal involvement and parenchymal atrophy occur most frequently in the left lateral segment and the right posterior segment. Significant caudate lobe hypertrophy may be seen. Postcontrast images may reveal heterogeneous enhancement. CCA may be seen as a complication of RPC.

Table 3 IgG4SC vs. PSC cholangiographic findings

	PSC	IgG4SC
Diverticulae	Classical, when present	Not seen
Strictures	Shorter, band like	Longer, lumen seen through thickened walls
Mural thickening > 2.5 mm	Rare	More likely
Prestenotic dilatation	Usually absent	May be seen
Distal CBD involvement	Less likely	More likely
Hepatic parenchymal changes	Signal changes and morphological changes may be seen	Usually absent

Abbreviations: CBD, common bile duct; IgG4SC, immunoglobulin G4-related sclerosing cholangitis; PSC, primary sclerosing cholangitis.

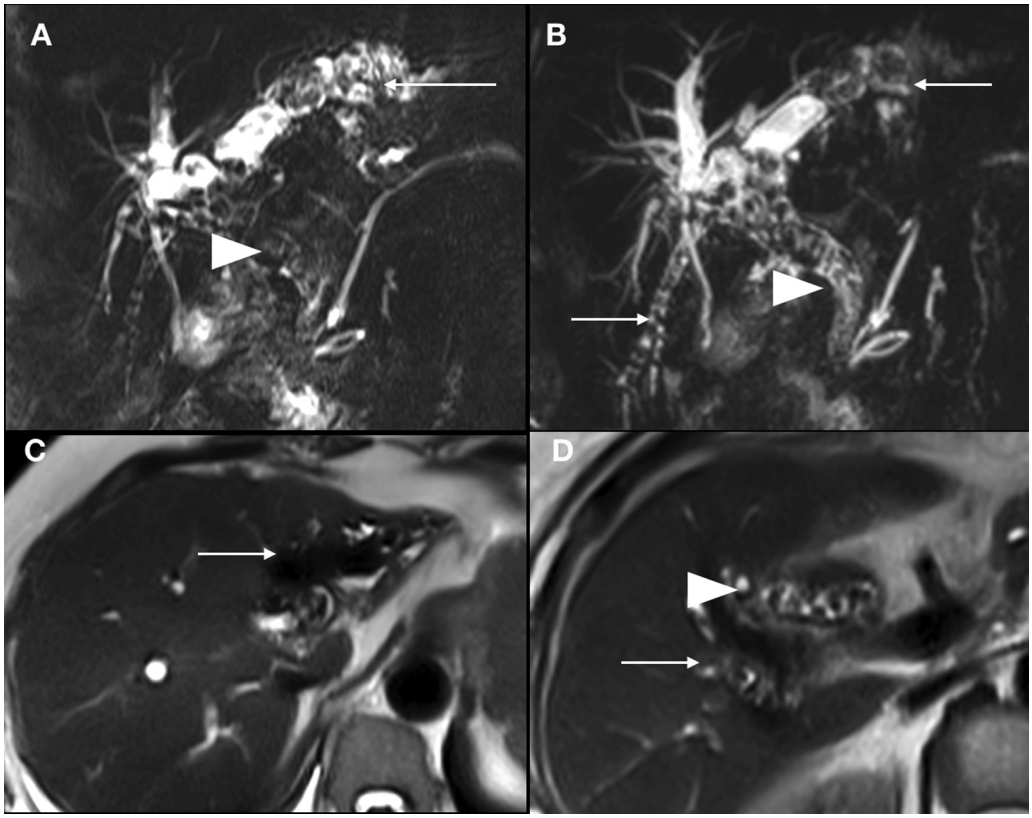

Fig. 12 Coronal magnetic resonance cholangiopancreatography (MRCP) images (**A**, **B**) and T2-weighted (T2W) axial images (**C**, **D**) in a 38-year-old patient with jaundice showing markedly dilated biliary radicles showing hypointense filling defects suggestive of calculi in the dilated biliary radicles (white arrows) and in the dilated common bile duct (CBD) (white arrowheads). Findings are suggestive of recurrent pyogenic cholangitis.

USG usually shows increased periportal echogenicity with marked ductal dilatation with intraductal calculi. Visualization of calculi is variable on CT; however, brown pigment stones of RPC are usually seen on CT. MRI is the imaging modality of choice and shows the imaging findings described above. Treatment consists of biliary drainage, surgical stone removal, or biliary bypass. Liver failure may occur, prompting transplantation.[47]

Biliary Parasites

Manifestations of parasitic infestation vary with the specific infestation and presence of eosinophilia, serology and stool examination may help clinch the diagnosis. The most common parasitic infestations include *Echinococcus granulosus*, which is seen initially as a unilocular cyst surrounded by a pericyst, or the typical spoke wheel appearance. Rupture or fistulization may occur with the biliary tree causing cholangitis and jaundice depending on the site of rupture. The imaging finding in that case is that of a focal defect in the wall of the cyst communicating with dilated biliary radicles which may also show cysts within on MRCP.

Ascariasis may be seen in the biliary tree, in the CBD, biliary radicles, or even GB. Ascaris worms on ultrasound are seen as parallel echogenic lines, on CT they are seen as somewhat hyperattenuating compared to bile, and on MRI they are seen as linear filling defects, hypointense on a

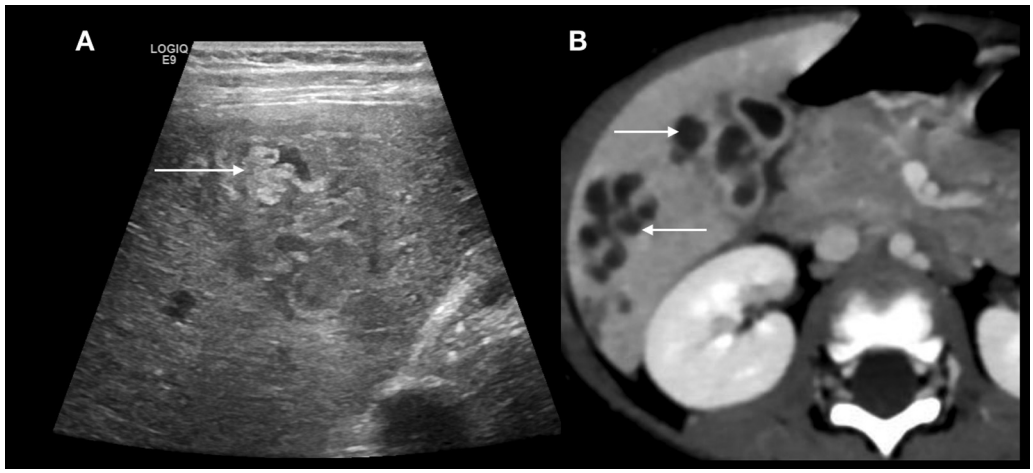

Fig. 13 A young female with fever and eosinophilia. Outside computed tomography (CT) report of liver abscesses. Follow-up CT was done followed by ultrasonography (USG). Transverse USG (**A**) image showing irregular heteroechoic track with echogenic central and marginal areas. Axial CT (**B**) showing irregular branching tracks in the right lobe of liver extending up to the hepatic margins (tunnels and caves sign). Findings are suggestive of hepatic Fascioliasis. Partial resolution was seen on anti-helminthic treatment.

background of bright bile. Biliary radicle dilatation may be seen and accompanying changes of AC may be seen as well.

Fasciola hepatica metacercariae perforate the duodenal wall and migrate into the peritoneal cavity, thereafter they penetrate the liver capsule and enter the hepatic parenchyma leading to clusters of sterile necrotic cavities and abscesses. They may be misdiagnosed as pyogenic abscesses. The flukes mate and start releasing eggs, which can cause biliary inflammation, wall thickening, and biliary radicle dilatation. CT may show the entire path of migration from the entry site to central liver with the "tunnels and caves" sign. Ultrasound may show the parasites and the serpentine echogenic tracks. MRI shows similar findings as CT[25,48] (►**Fig. 13**).

Acquired Immunodeficiency Syndrome-Related Cholangitis

Acquired immunodeficiency syndrome-related cholangitis, also known as human immunodeficiency virus cholangiopathy, is seen in patients with a CD4 count of less than 100 cells/mm^3. The prevalence has reduced due to highly active antiretroviral therapy. The underlying mechanisms is possibly related to opportunistic biliary infections.[49] Four types of appearances have been described—type I - papillary stenosis, type II - intrahepatic SC-like pattern, type III - intrahepatic involvement with papillary stenosis, most common type, and type IV - long extrahepatic bile duct strictures with or without intrahepatic involvement.[49,50] MRI is the imaging modality of choice and can show the above findings. USG can show ductal dilatation (►**Fig. 14**).

Ischemic Cholangitis

Ischemic cholangitis arises due to compromise of the hepatic artery supply. These are most commonly seen in posttransplant patients with hepatic artery thrombosis (HAT). Polyarteritis nodosa and giant cell arteritis are some of the primary arterial pathologies which may cause ischemic cholangitis. Disorders such as paroxysmal nocturnal hemoglobinuria, sickle cell anemia, and hereditary hemorrhagic

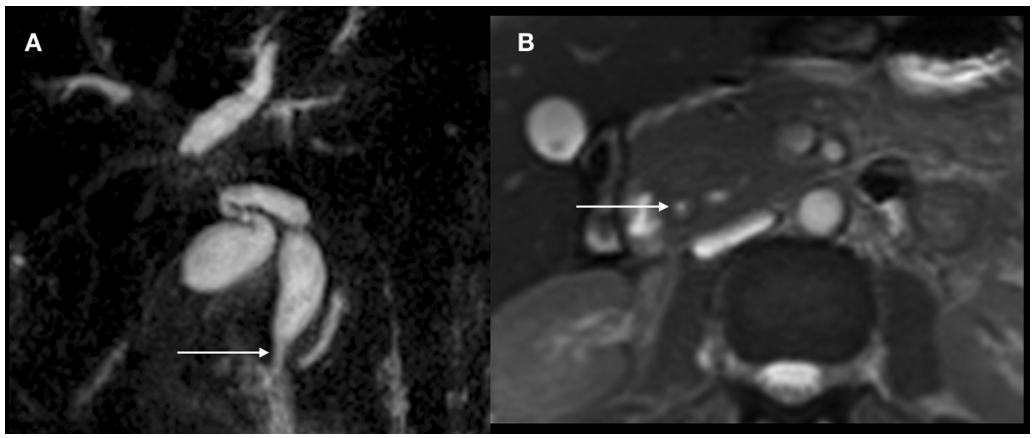

Fig. 14 Young male with jaundice, known human immunodeficiency virus (HIV) positive. Coronal three-dimensional (3D) magnetic resonance cholangiopancreatography (MRCP) thin slab image (**A**) showing narrowing at the lower end of the common bile duct (CBD) (arrow) with dilatation of the intrahepatic biliary radicle dilatation consistent with HIV cholangiopathy. Axial T2-weighted (T2W) images (**B**) showing circumferential thickening of lower end of the CBD.

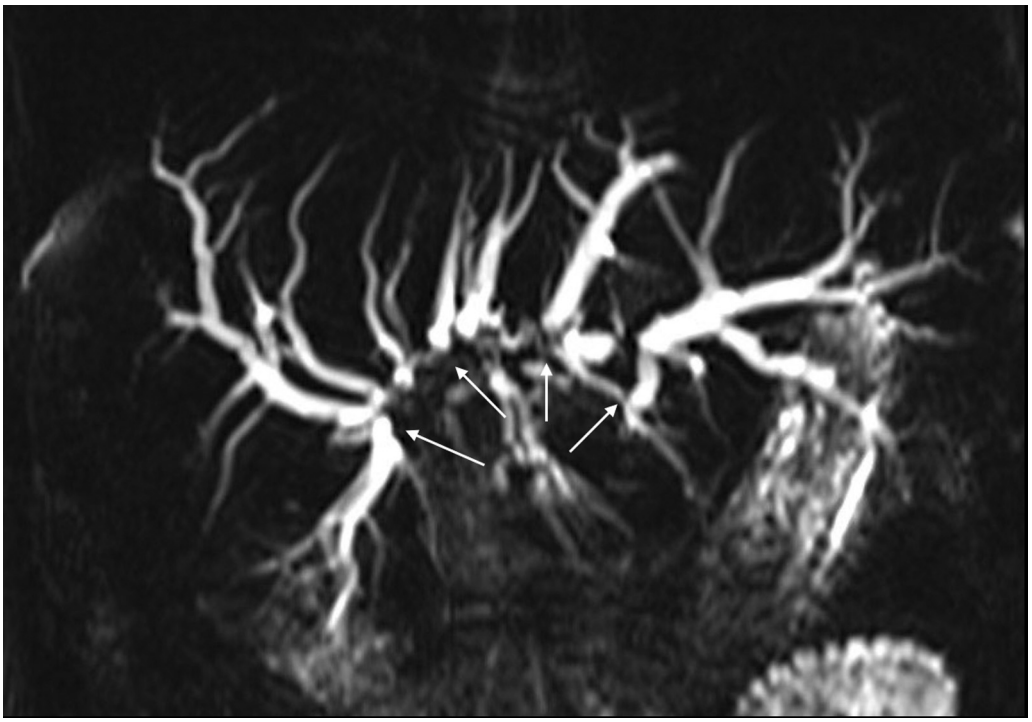

Fig. 15 Coronal magnetic resonance cholangiopancreatography (MRCP) images in a 4-year-old male child with hepatic artery thrombosis showing multiple irregular nonanastomotic strictures on follow-up (arrows). Findings consistent with ischemic cholangiopathy.

telangiectasia may cause ischemic cholangitis. Ischemia is believed to be the cause for chemotherapy-associated cholangitis caused by drugs which include floxuridine and arterial chemotherapeutic agents, regardless of the agents used, including 5-fluorouracil, cisplatin, paclitaxel, mitomycin C, and Yttrium-90.[51]

In the acute stages, desquamation of the biliary epithelium occurs which leads to the formation of biliary casts, followed by obstruction and dilatation of the bile ducts. Casts appear hyperintense on T1W images and tend to be linear and branching which may help differentiate them from calculi. Severe insults can cause transmural biliary necrosis and breakdown followed by formation of bilomas and abscesses. If the patient survives the acute event, then multiple irregular strictures may form accompanied by variable biliary dilatation which may give a PSC-like picture; however, the strictures tend to be Hilar or mid-CBD in location. Biliary dilatation and abscesses along with areas of breakdown are readily seen on USG, MR, and CT. CT angiography is most commonly used to confirm HAT. Hepatic artery patency may also be evaluated by color Doppler or MR angiography. Drainage procedures including percutaneous biliary drainages and cast removals may be done for symptom mitigation of these patients; however, posttransplant HAT patients will require retransplant[2,31,51] (►**Fig. 15**).

Secondary Sclerosing Cholangitis in Critically Ill Patients

Secondary sclerosing cholangitis is a relatively recently recognized entity in patients receiving intensive care unit (ICU) treatment. It presents as a cholestatic liver disease in patients without history of hepatobiliary disease in critically ill patients due to a variety of conditions including polytrauma, burns, major surgery, and acute respiratory distress syndrome including coronavirus disease pneumonia. The diagnosis is one of exclusion in the correct clinical context. The course is usually severe and progressive with a high mortality. The most accepted causative theory proposes a combination of ischemia along with changes in bile composition leading to necrosis with cast formation.[52,53]

Ultrasound is not a sensitive test.[52] Early MRI may show presence of biliary casts later on progressing to strictures, biliary wall thickening, and progressive destruction of the peripheral bile ducts. Imaging findings of biliary casts in an ICU patient are suggestive of this entity. Delayed scans reveal pruned tree appearance with persistence of only the central biliary tree typical up to the second order ducts. ERCP is the gold standard. Associated findings include acalculous cholecystitis, GB rupture, and liver abscess formations.[2]

Treatment includes biliary drainage and antibiotic therapy. In patients with biliary cirrhosis, liver transplant is the only curative procedure.[53]

Biliary Strictures

Biliary strictures often present a diagnostic challenge during preoperative evaluation to determine their benign or malignant nature. Benign biliary strictures are secondary to a wide spectrum of etiologies; however, the key is to be able to differentiate benign from malignant etiologies (►**Table 4**).[54–57]

In the absence of a mass on imaging, ERCP is the next modality that permits stricture assessment, tissue sample acquisition, and biliary drainage. Strictures with negative or

Table 4 Malignant vs. benign biliary stricture

	Malignant	Benign
Length of involvement	Long stenosis > 12 mm	Short segment
Duct wall thickness	Wall thickness > 3 mm	Wall thickness < 3 mm
Duct wall enhancement	Hyperenhancement of ductal wall on portal venous phase images	Absence of hyperenhancement
Stricture morphology	Asymmetrical wall thickening with luminal irregularity and shouldering	Smooth concentric narrowing
Outer margins	Indistinct outer margins of involved bile duct wall	Smooth outer margin
Presence of diffusion restriction	Presence of diffusion restriction	Absence of diffusion restriction

inconclusive brush cytology and transpapillary biopsies are defined as "indeterminate biliary strictures" and an additional cholangioscopy for visual impression and targeted biopsies is recommended at a subsequent ERCP.[58]

Distal CBD strictures can be targeted by alternate approaches including EUS and percutaneous cholangioscopies with subsequent fine-needle aspiration/biopsy. In patients with negative visual assessment as well as tissue diagnosis, serial follow-up with cross-sectional imaging for at least 6 months is recommended before considering benign etiology.[59]

Conclusion

A wide variety of benign diseases can involve the biliary system, some of which may have only subtle differences in the imaging findings. Though ultrasound is the first imaging modality to be used in a suspected case of obstructive jaundice or suspected cholangiopathy, CT may help to visualize cholangiopathies and may show many similar findings as MRI; however, CE MRI along with MRCP should be used for comprehensive evaluation of biliary diseases. The radiologist, however, should also be aware of the pitfalls and differential diagnoses of the various MRI and cholangiographic findings, many of which may overlap.

Conflict of Interest
None declared.

Bibliography

1 Hu R, Hu R, Pandol Stephen. Physiology of the biliary tree. In: Surgical Disease of the Pancreas and Biliary Tree. Springer September 27–43, 2018. Doi: 10.1007/978-981-10-8755-4_2
2 Pria HD, Torres US, Faria SC, et al. Practical guide for radiological diagnosis of primary and secondary sclerosing cholangitis. Semin Ultrasound CT MRI 2022;43(06):490–509
3 Sundaram KM, Morgan MA, Itani M, Thompson W. Imaging of benign biliary pathologies. Abdom Radiol (NY) 2023;48(01):106–126
4 Abou-Khalil JE, Bertens KA. Embryology, anatomy, and imaging of the biliary tree. Surg Clin North Am 2019;99(02):163–174
5 Rozel C, Garel L, Rypens F, et al. Imaging of biliary disorders in children. Pediatr Radiol 2011;41(02):208–220
6 Mortelé KJ, Ros PR. Anatomic variants of the biliary tree: MR cholangiographic findings and clinical applications. Am J Roentgenol 2001;177(02):389–394
7 Bowie JD. What is the upper limit of normal for the common bile duct on ultrasound: how much do you want it to be? Am J Gastroenterol 2000;95(04):897–900
8 Wills M, Harvey CJ, Kuzmich S, Afaq A, Cosgrove D. Ultrasound of the gall bladder and biliary tree: part 1. Br J Hosp Med (Lond) 2014;75(06):312–317
9 Rubens DJ. Ultrasound imaging of the biliary tract. Ultrasound Clin 2007;2(03):391–413
10 Park SJ, Han JK, Kim TK, Choi BI. Three-dimensional spiral CT cholangiography with minimum intensity projection in patients with suspected obstructive biliary disease: comparison with percutaneous transhepatic cholangiography. Abdom Imaging 2001;26(03):281–286
11 Morosi C, Civelli E, Battiston C, et al. CT cholangiography: assessment of feasibility and diagnostic reliability. Eur J Radiol 2009;72 (01):114–117
12 Molvar C, Glaenzer B. Choledocholithiasis: evaluation, treatment, and outcomes. Semin Intervent Radiol 2016;33(04):268–276
13 Welle CL, Miller FH, Yeh BM. Advances in MR imaging of the biliary tract. Magn Reson Imaging Clin N Am 2020;28(03):341–352
14 Katabathina VS, Dasyam AK, Dasyam N, Hosseinzadeh K. Adult bile duct strictures: role of MR imaging and MR cholangiopancreatography in characterization. Radiographics 2014;34(03): 565–586
15 Sanders DJ, Bomman S, Krishnamoorthi R, Kozarek RA. Endoscopic retrograde cholangiopancreatography: current practice and future research. World J Gastrointest Endosc 2021;13(08): 260–274
16 Napolitano M, Franchi-Abella S, Damasio MB, et al. Practical approach to imaging diagnosis of biliary atresia, Part 1: prenatal ultrasound and magnetic resonance imaging, and postnatal ultrasound. Pediatr Radiol 2021
17 Kim YH, Kim MJ, Shin HJ, et al. MRI-based decision tree model for diagnosis of biliary atresia. Eur Radiol 2018;28(08):3422–3431
18 Todani T. Congenital choledochal dilatation: classification, clinical features, and long-term results. J Hepato Biliary Pancreat Surg 1997;4:276–282
19 Lewis VA, Adam SZ, Nikolaidis P, et al. Imaging of choledochal cysts. Abdom Imaging 2015;40(06):1567–1580
20 Kamisawa T, Ando H, Hamada Y, et al; Japanese Study Group on Pancreaticobiliary Maljunction. Diagnostic criteria for pancreaticobiliary maljunction 2013. J Hepatobiliary Pancreat Sci 2014;21 (03):159–161
21 Bali MA, Pezzullo M, Pace E, Morone M. Benign biliary diseases. Eur J Radiol 2017;93:217–228

22 Griffin N, Yu D, Alexander Grant L. Magnetic resonance cholangiopancreatography: pearls, pitfalls, and pathology. Semin Ultrasound CT MR 2013;34(01):32–43
23 Prabhakar PD, Prabhakar AM, Prabhakar HB, Sahani D. Magnetic resonance cholangiopancreatography of benign disorders of the biliary system. Magn Reson Imaging Clin N Am 2010;18(03): 497–514, xi
24 Meeralam Y, Al-Shammari K, Yaghoobi M. Diagnostic accuracy of EUS compared with MRCP in detecting choledocholithiasis: a meta-analysis of diagnostic test accuracy in head-to-head studies. Gastrointest Endosc 2017;86(06):986–993
25 Catalano OA, Sahani DV, Forcione DG, et al. Biliary infections: spectrum of imaging findings and management. Radiographics 2009;29(07):2059–2080
26 Pötter-Lang S, Ba-Ssalamah A, Bastati N, et al. Modern imaging of cholangitis. Br J Radiol 2021;94(1125):20210417
27 Kiriyama S, Kozaka K, Takada T, et al. Tokyo Guidelines 2018: diagnostic criteria and severity grading of acute cholangitis (with videos). J Hepatobiliary Pancreat Sci 2018;25(01):17–30
28 Dhiman RK, Saraswat VA, Valla DC, et al. Portal cavernoma cholangiopathy: consensus statement of a working party of the Indian national association for study of the liver. J Clin Exp Hepatol 2014;4(Suppl 1):S2–S14
29 Moomjian LN, Winks SG. Portal cavernoma cholangiopathy: diagnosis, imaging, and intervention. Abdom Radiol (NY) 2017; 42(01):57–68
30 Shin SM, Kim S, Lee JW, et al. Biliary abnormalities associated with portal biliopathy: evaluation on MR cholangiography. AJR Am J Roentgenol 2007;188(04):W341-7
31 Seo N, Kim SY, Lee SS, et al. Sclerosing cholangitis: clinicopathologic features, imaging spectrum, and systemic approach to differential diagnosis. Korean J Radiol 2016;17(01):25–38
32 Bowlus CL, Arrivé L, Bergquist A, et al. AASLD practice guidance on primary sclerosing cholangitis and cholangiocarcinoma. Hepatology 2023;77(02):659–702
33 Khoshpouri P, Habibabadi RR, Hazhirkarzar B, et al. Imaging features of primary sclerosing cholangitis: from diagnosis to liver transplant follow-up. Radiographics 2019;39(07):1938–1964
34 European Association for the Study of the Liver. Electronic address: easloffice@easloffice.eu European Association for the Study of the Liver. Electronic address: easloffice@easloffice.eu; European Association for the Study of the Liver. EASL Clinical Practice Guidelines on sclerosing cholangitis. J Hepatol 2022;77 (03):761–806
35 Venkatesh SK, Welle CL, Miller FH, et al; IPSCSG. Reporting standards for primary sclerosing cholangitis using MRI and MR cholangiopancreatography: guidelines from MR Working Group of the International Primary Sclerosing Cholangitis Study Group. Eur Radiol 2022;32(02):923–937
36 Ruiz A, Lemoinne S, Carrat F, Corpechot C, Chazouillères O, Arrivé L Radiologic course of primary sclerosing cholangitis: assessment by three-dimensional magnetic resonance cholangiography and predictive features of progression. Hepatology 2014;59(01):242–250
37 Madhusudhan KS, Das P, Gunjan D, Srivastava DN, Garg PK. IgG 4-related sclerosing cholangitis: a clinical and imaging review. AJR Am J Roentgenol 2019;213(06):1221–1231
38 Kamisawa T, Funata N, Hayashi Y, et al. A new clinicopathological entity of IgG4-related autoimmune disease. J Gastroenterol 2003; 38(10):982–984
39 Ghazale A, Chari ST, Zhang L, et al. Immunoglobulin G4-associated cholangitis: clinical profile and response to therapy. Gastroenterology 2008;134(03):706–715
40 Nakazawa T, Naitoh I, Hayashi K, et al. Diagnostic criteria for IgG 4-related sclerosing cholangitis based on cholangiographic classification. J Gastroenterol 2012;47(01):79–87
41 Nakazawa T, Kamisawa T, Okazaki K, et al. Clinical diagnostic criteria for IgG4-related sclerosing cholangitis 2020: (Revision of the clinical diagnostic criteria for IgG4-related sclerosing cholangitis 2012). J Hepatobiliary Pancreat Sci 2021;28(03):235–242
42 Hafezi-Nejad N, Singh VK, Fung C, Takahashi N, Zaheer A. MR imaging of autoimmune pancreatitis. Magn Reson Imaging Clin N Am 2018;26(03):463–478
43 Nakazawa T, Ohara H, Sano H, Ando T, Joh T. Schematic classification of sclerosing cholangitis with autoimmune pancreatitis by cholangiography. Pancreas 2006;32(02):229
44 Ludwig DR, Anderson MA, Itani M, Sharbidre KG, Lalwani N, Paspulati RM. Secondary sclerosing cholangitis: mimics of primary sclerosing cholangitis. Abdom Radiol (NY) 2023;48(01): 151–165
45 O'Brien C, Malik M, Jhaveri K. MR imaging in primary sclerosing cholangitis and other cholangitis. Radiol Clin North Am 2022;60 (05):843–856
46 Wani NA, Robbani I, Kosar T. MRI of oriental cholangiohepatitis. Clin Radiol 2011;66(02):158–163
47 Kwan KEL, Shelat VG, Tan CH. Recurrent pyogenic cholangitis: a review of imaging findings and clinical management. Abdom Radiol (NY) 2017;42(01):46–56
48 Lim JH, Mairiang E, Ahn GH. Biliary parasitic diseases including clonorchiasis, opisthorchiasis and fascioliasis. Abdom Imaging 2008;33(02):157–165
49 Tonolini M, Bianco R. HIV-related/AIDS cholangiopathy: pictorial review with emphasis on MRCP findings and differential diagnosis. Clin Imaging 2013;37(02):219–226
50 Bilgin M, Balci NC, Erdogan A, Momtahen AJ, Alkaade S, Rau WS. Hepatobiliary and pancreatic MRI and MRCP findings in patients with HIV infection. AJR Am J Roentgenol 2008;191(01):228–232
51 Alabdulghani F, Healy GM, Cantwell CP. Radiological findings in ischaemic cholangiopathy. Clin Radiol 2020;75(03):161–168
52 Martins P, Verdelho Machado M. Secondary sclerosing cholangitis in critically ill patients: an underdiagnosed entity. GE Port J Gastroenterol 2020;27(02):103–114
53 Gudnason HO, Björnsson ES. Secondary sclerosing cholangitis in critically ill patients: current perspectives. Clin Exp Gastroenterol 2017;10:105–111
54 Song J, Li Y, Bowlus CL, Yang G, Leung PSC, Gershwin ME. Cholangiocarcinoma in patients with primary sclerosing cholangitis (PSC): a comprehensive review. Clin Rev Allergy Immunol 2020;58(01):134–149
55 Yang T, Wei H, Chen J, Jiang H, Chen Y, Song B. The value of contrast-enhanced magnetic resonance imaging for diagnosis of extrahepatic cholangiocarcinoma. Heliyon 2023;10(01):e23448
56 Kim JY, Lee JM, Han JK, et al. Contrast-enhanced MRI combined with MR cholangiopancreatography for the evaluation of patients with biliary strictures: differentiation of malignant from benign bile duct strictures. J Magn Reson Imaging 2007;26(02):304–312
57 Park HJ, Kim SH, Jang KM, Choi SY, Lee SJ, Choi D. The role of diffusion-weighted MR imaging for differentiating benign from malignant bile duct strictures. Eur Radiol 2014;24(04):947–958
58 Angsuwatcharakon P, Kulpatcharapong S, Moon JH, et al. Consensus guidelines on the role of cholangioscopy to diagnose indeterminate biliary stricture. HPB (Oxford) 2022;24(01):17–29
59 Ayoub F, Othman MO. Guidelines on cholangioscopy for indeterminate biliary strictures: one step closer to consensus. Hepatobiliary Surg Nutr 2023;12(05):776–779

